This is a preprint, the final version is subject to change, of the American Mineralogist (MSA)
Cite as Authors (Year) Title. American Mineralogist, in press.
(DOI will not work until issue is live.) DOI: http://dx.doi.org/10.2138/am.2014.4848

Final accepted version

The occurrence of platinum-group element and gold minerals in the Bon Accord Ni-oxide body, South Africa

FEDERICA ZACCARINI [1,*], MARIAN TREDOUX [2], DUNCAN E. MILLER [2], GIORGIO GARUTI [1], THOMAS AIGLSPERGER [3], JOAQUIN A. PROENZA [3]

[1]Department of Applied Geosciences and Geophysics, University of Leoben, A 8700 Leoben, Austria
[2]Department of Geology, University of the Free State, Bloemfontein 9300, South Africa
[3]Department of Crystallography, Mineralogy and Ore Deposits, University of Barcelona, Spain

*E-mail: federica.zaccarini@unileoben.ac.at

ABSTRACT

Two samples from the enigmatic Ni-oxide body of Bon Accord (Barberton greenstone belt, South Africa) have been investigated with the hydroseparation technique in order to obtain heavy mineral concentrates. The concentrates contain abundant Pt, Pd and gold minerals never reported before from the Bon Accord Ni-oxide body. The grains occur as: i) minute inclusions (<3 micrometers) in trevorite (ideally $NiFe^{3+}O_4$) and ii) larger (5–70 micrometers) free aggregates liberated from the host phase. The first group comprises a number of PGM compounds of Pd-Sb, Pd-Sb-As, Pd-Cu-Sb, Pt-Sb, Pt-As-S, Ru-As-S, Ru-S, along with free grains of Ni-Fe-As. The second consists of sperrylite ($PtAs_2$), members of the sobolevskite-kotulskite series, and electrum. These results are in good agreement with previous analyses of PGE-Au in bulk rock. Paragenetic relationships indicate that the PGM and electrum are of secondary origin, probably generated during low-temperature metamorphism of the Ni-rich mineralization. They have a terrestrial origin and are related with a low-sulfidation regime that usually accompanies

Always consult and cite the final, published document. See http://www.minsocam.org or GeoscienceWorld

hydrothermally driven serpentinization of mafic-ultramafic bodies. The ligands in the newly formed PGM (As, Sb, Bi, Te, O) probably proceed from the same source of the hydrothermal solutions. In this model, the metals Ni-PGE-Au were original components of the primary mineral assemblage of the Bon Accord precursor, whereas As, Sb, Bi, Te, O might have been contributed by the metasomatizing fluids, during near-surface evolution of the ore body. The data on the high-grade heavy mineral concentrates, obtained by hydroseparation, have provided new knowledge about the mineral deportment of Pd, Pt and Au.

Keywords: Platinum-group minerals, gold minerals, Bon Accord Ni-oxide body, hydroseparation, heavy mineral concentrate, Barberton greenstone, South Africa

INTRODUCTION

Platinum-group minerals (PGM) are the carriers of the platinum-group elements (PGE): osmium (Os), iridium (Ir), ruthenium (Ru), rhodium (Rh), platinum (Pt) and palladium (Pd). These elements, with a concentration of about 10^{-6} to 10^{-10}% in the Earth's crust, are numbered among the ultra-trace elements. They occur naturally as alloys, native elements or in combination with other elements, mainly S, As, Te, Bi, Sb, Hg, Se, Sn (see Cabri 2002) and more rarely with O (Cabri et al. 1981; Garuti et al. 1997; Garuti and Zaccarini, 1997; Jedwab and Cassedanne 1998; McDonald et al. 1999; Uysal et al. 2009). PGM are rare, representing less than 3% of the minerals approved by the Commission on New Minerals and Mineral Names of the International Mineralogical Association (IMA). According to Daltry and Wilson (1997), only 96 phases containing the PGE as major components were approved before 1997. These authors also listed more than 500 different chemical compositions of PGE-bearing phases that, very likely, correspond to new mineral species. However, since 1997, only 28 new PGM have been approved (Barkov et al. 2002a;b; Cabri 2002; Stanley et al. 2002; Paar et al. 2004; 2005; Rudashevsky et al. 2004; Cabri et al. 2005b; McDonald et al. 2005; 2010; Botelho et al. 2006; Kojonen et al. 2007; Mochalov et al. 2007; Yu et al. 2009; Vymazalova et al. 2009; 2012a;b). The failure in the identification of PGM is due mainly to their mode of occurrence as minute inclusions (usually less than 100 micrometers in size) which are randomly distributed in their host rocks, thus severely limiting conventional crystallographic characterization by X-ray spectrometry, as

Always consult and cite the final, published document. See http://www.minsocam.org or GeoscienceWorld

discussed below.

Traditionally the PGM are located on polished section by reflected light or electron microscope and investigated *in situ*. Usually, the identification of the mineral species cannot be done on a simple determination of the optical properties owing to the small size of grains, and is dependent on the use of electron microprobe analysis. Furthermore, although the *in situ* study provides useful information on paragenetical relationships of the PGM, it commonly does not allow a complete picture of their abundance and distribution throughout their host rock. Polished sections represent only a small portion of the host rocks, and it is known that two-dimensional counting of three-dimensionally distributed grains in solids may produce statistically deficient results (Oberthür et al. 2008; Cabri 2012; Shi et al. 2013). This is particularly critical when the subsidiary phases are unevenly dispersed and occupy extremely small volumes within the host, and for this reason they can be easily missed in any particular section. To remedy these problems, an innovative hydroseparation technique able to extract the PGM from their matrix, and concentrate them, has been recently applied successfully to a number of natural occurrences (Rudashevsky et al. 2002; 2004; Cabri et al. 2005a;b; Grammatikopoulos et al. 2007; Kapsiotis et al. 2009; Zaccarini et al. 2009; McDonald et al. 2010).

This paper reports on the discovery of a complex PGM and gold assemblage, obtained by application of the hydroseparation technique to a suite of samples from the enigmatic Bon Accord Ni-oxide body (Mpumalanga Province, South Africa). Internal texture and composition of encountered minerals have been documented through detailed study by field emission electron microscopy (FE-SEM) and electron microprobe analyses.

PREVIOUS STUDIES ON BON ACCORD

The Bon Accord Ni-oxide body was discovered in the 1920s, in the northwestern sector of the Archaean Barberton greenstone belt. It attracted attention because of its unusually high (>35% whole rock) NiO values (Trevor 1920; Walker 1923; Partridge 1944), and the entire mass was removed for processing, leaving a hole approximately 6 m^3 in size (De Waal 1978). After the disappointing discovery that the material was too refractory to smelt, the ore was discarded as waste about 3 km from the original outcrop location. Unfortunately, none of the material was left *in situ*.

Always consult and cite the final, published document. See http://www.minsocam.org or GeoscienceWorld

The origin of the Bon Accord Ni-oxide body has been debated for three decades. De Waal (1978) interpreted it as an oxidized remnant of an Archaean iron meteorite, while Tredoux et al. (1989) proposed that it is a strongly altered deep mantle fragment within the mantle section of the Archaean Jamestown ophiolite described by de Wit et al. (1987): Mineral chemical similarities between chromite grains in the Bon Accord Ni-rich mineralization and those in the surrounding ultramafite, which they interpreted as being suggestive of a cogenetic history, prompted Tredoux et al. (1989) to reject the meteorite hypothesis of De Waal (1978). The terrestrial nature of the Bon Accord Ni-oxide body was supported recently by Cr isotopic data (Tredoux et al. 2013), but proof of a deep mantle origin remains elusive.

Besides the high concentrations of Ni, the Bon Accord Ni-oxide body is also enriched in PGE and contains appreciable amount of Au (Tredoux et al. 1989) (Table 1). However, to date only three grains of ruthenium, less than two micrometers in size (Fig. 1), have been discovered in the Bon Accord Ni-oxide body using traditional petrographic methodology (Tredoux et al. 2014, submitted). The data presented in this paper demonstrate that the PGM assemblage is much more complex then previously supposed, and that the PGM are accompanied by significant amount of gold. This new information is used to bring more light to the origin of this intriguing mineralization.

SAMPLE DESCRIPTION AND METHODOLOGY

The samples used for this investigation were collected in the 1980s by one of the authors (MT) from an abandoned core shed near the hole from which the ore body was removed. The studied samples, called NCH and NCN, originally formed part of the schistose outer rim of the Bon Accord Ni-oxide body (Tredoux et al. 1989; Tredoux et al. 2013). The samples are dominantly composed of nepouite and willemseite, after the olivine liebenbergite, with stringers and clumps of the Ni-spinel trevorite making up about 30% of the mineralogy (for explanations of the Ni-rich minerals in the Bon Accord Ni-oxide body, see de Waal 1972; 1978; 1979; de Waal and Calk 1973). As only a few hand specimens from Bon Accord Ni-oxide body are now available for study, only 830 grams of sample were used during the present investigation.

The material was crushed for 15 seconds with a swing mill, using a carbon steel bowl, and then sieved into the following fractions: +53 micrometers, <53 micrometers, 75 micrometers

Always consult and cite the final, published document. See http://www.minsocam.org or GeoscienceWorld

and 106 micrometers. From these fractions, a heavy minerals concentrate was obtained at Barcelona University (Spain) using the HS 11 hydroseparator instrument and following the procedure recently described in several papers (Cabri et al. 2005a;b; Grammatikopoulos et al. 2007; Rudashevsky et al. 2002; 2004). The concentrates were mounted in epoxy blocks and polished for mineralogical examination. Four polished blocks of one inch in diameter were obtained for each concentrate. The PGM and gold were located by scanning the polished blocks in part using the JEOL field emission electron microscope (FE-SEM) installed at the Barcelona University (Spain), and the JEOL JXA-8200 available at the Eugen F. Stumpfl Electron Microprobe Laboratory at the Leoben University (Austria). Selected PGM and gold grains with a size of more than five micrometers were analyzed quantitatively by the wavelength dispersive (WD) system at the Eugen F. Stumpfl Electron Microprobe Laboratory.

The gold minerals were analyzed using at 25kV accelerating voltage and 30nA beam current. The counting times for peak and background were 20 and 10 seconds for Au and Ag, and were increased up to 60 and 30 seconds in the analysis of trace elements. Under these conditions low detection limits were achieved for As (270 ppm), S (150 ppm), Fe (80 ppm), Co (70 ppm), Cu (120 ppm), Ni (100 ppm), Zn (140 ppm), Se (180 ppm), Sb (190 ppm), Bi (370 ppm), Hg (550 ppm), and Te (80 ppm). Sulfur, Cu, Ni, Fe, Co and Zn were analyzed using the Kα lines, As, Ag, Se, Sb and Te using Lα and Au, Bi, Hg using Mα. The following analyzing crystals were used: TAP for As and Se, PETJ for S, Sb, Bi, Ag, Au and Hg, PETH for Te, and LIFH for Fe, Ni, Co, Zn and Cu. Natural, chalcopyrite, millerite, skutterudite, stibnite, calaverite, sphalerite, and synthetic electrum, CuSe, Bi_2Te_3 and Pd_3HgTe_3 were used as reference material.

The quantitative analyses of PGM were performed using 20kV accelerating voltage and 10nA beam current. The counting times for peak and background were 20 and 10 seconds, respectively. Pure metals were the reference material for Os, Ir, Ru, Rh, Pt and Pd. The natural minerals chalcopyrite, galena, and synthetic nickeline and Bi_2Te_3 were used to calibrate Cu, Fe, S, Pb, Ni, As, Bi, and Te. The following X-ray lines were used: Kα for S, Fe, Cu and Ni; Lα for Ir, Ru, Rh, Pt, Pd, As and Te; and Mα for Os, Bi and Pb. The following diffracting crystals were selected: TAP for As, PETJ for S, Bi, Pb and Te, PETH for Ru, Os, Rh, LIFH for Ni, Cu, Ir and Pt.

Only qualitative EDS analyses could be performed for the PGM which has very small size (generally less than one micron), and in those case where they occur as minute intergrowth of

Always consult and cite the final, published document. See http://www.minsocam.org or GeoscienceWorld

two or more phases.

RESULTS

The precious minerals were encountered only in the +53 micrometers, <53 micrometers concentrates and they consist of PGM and electrum. The fractions 75 micrometers and 106 micrometers proved to be barren. They occur as: i) minute inclusions (<3 micrometers) of various PGM in trevorite (Figs 2, 3), ii) large (5–70 micrometers) free grains of PGM and electrum liberated from the host phase (Figs 4, 5).

The grains included in trevorite may consist of a single phase (Fig. 3), or form composite aggregates of two or more PGM (Figs 2A, B, C, D, E). According to the EDS spectra, they comprise PGM compounds of Pd-Sb, Pd-Sb-As, Pd-Cu-Sb, Pt-Sb, Pt-As-S, Ru-As-S, Ru-S, along with several grains of Ni-Fe-As (Fig. 2F). Although their small size prevents any unequivocal mineralogical classification, the EDS data suggest possible attribution of the Pd-Sb PGM to the following ideal species: stibiopalladinite (Pd_5Sb_2), naldrettite (Pd_2Sb), ungavaite (Pd_4Sb_3) and sudburyite (Pd,Sb). The Pt bearing PGM probably corresponded to genkinite ($(Pt,Pd)_4Sb_3$) or platarsite (PtAsS). The grains containing Ru and S very likely were laurite (RuS_2) and ruarsite (RuAsS). The Ni-Fe compounds may correspond to one of the phases described by Tredoux et al. (2014, submitted).

Most of the free grains could be properly classified using electron microprobe quantitative analyses. They comprise electrum (Table 2) and the PGM sperrylite, $PtAs_2$ (Table 3), sobolevskite, PdBi, and a Bi-rich kotulskite, PdTe (Table 4). Gold phases are very abundant in the concentrates NC-H and very rare in those obtained from the NC-N sample. Electrum usually occur as single-phase crystals varying in size from 5 up to 60 micrometers (Figs 4A, B, C) and only one grain was found associated with sperrylite (Figs 4E, F). The composition is almost homogenous with Ag concentrations between 26.64 and 29.11 wt% (Table 2). Among the trace elements analyzed in the gold grains, Co, Zn, Sb, As, Hg and Se are always below detection limit, and the contents of S, Ni and Te are very low (up to 0.07 wt%, 0.09 wt% and 0.08 wt%, respectively). Appreciable amounts of Fe (up to 0.71 wt%), Cu (up to 0.19 wt%), Bi (up to 0.49 wt%) have been detected (Table 2).

Sperrylite was found to be particularly abundant in sample NC-H, mostly occurring as

Always consult and cite the final, published document. See http://www.minsocam.org or GeoscienceWorld

single-phase grains of 10 to 70 micrometers in size (Figs 4A, B, C). Electron microprobe analyses show trace amounts of S, Os, Ir, Ru, Rh, Pt, and Pd. The sperrylite associated with gold (Figs 4E, F) is distinguished by slight higher Fe (2.49 wt%) and Rh (1.1 wt%) contents, while it is depleted in Os, Ir and Ru (below detection limit) (Table 3). Sobolevskite and the Pd-Te-Bi compound occur exclusively in the concentrates of the NC-N sample. They form single-phase crystals with sizes which vary from 5 to about 30 micrometers (Fig. 5). The Bon Accord sobolevskite appears to have rather pure composition PdBi with weak substitution of Fe up to 9.67 at% (Table 4). On the basis of its composition of the Pd-Te-Bi mineral can classified ad Bi-rich kotulskite, with 2.52 at% Fe. The two compositions are plotted on the ternary diagram Pd-Te-Bi (Fig. 6), and compared with phases of the sobolevskite-kotulskite solid solution, reported from various localities worldwide and compiled by Cook et al. (2002). The sobolevskite from Bon Accord roughly correspond to the PdBi end-member reported from Norilsk (Evstigneeva and Kovalenker 1975), whereas the Pd-Bi-Te has intermediate composition between PdBi and PdTe, compatible with experimental results (Vymazalova et al. 2013) and resembles PGM reported from Norilsk (Kovalenker et al. 1975), Two Duck Lake (Watkinson and Ohnenstetter 1992), Lukkulaisvaara (Groshovskaya et al. 1992) and Great Dyke (Coghill and Wilson 1993). This phase corresponds to a Bi-rich kotulskite.

DISCUSSION

Relationships between mineralogy and geochemistry

The Bon Accord Ni-oxide body is characterized by anomalous concentrations of Ni, Sb (and to a lesser extent As) and by very low amount of S (Tredoux et al. 1989). Tredoux et al. (2014, submitted) have recognized, in the Bon Accord Ni-oxide body, a set of phases that possibly represent new minerals in the Ni-Sb-As system: Ni_3Sb, Ni_5Sb_2, Ni_7Sb_3, $Ni_{11}Sb_8$, $Ni_3(As,Sb)$, $Ni_5(As,Sb)_2$ and $Ni_7(As,Sb)_3$. Few Ni bearing sulfides have been also observed during this investigation. All these mineralogical observations are fully consistent with the geochemical signature of the Bon Accord Ni-oxide body.

The Bon Accord samples are also enriched in PGE, up to more than 7000 ppb of total PGE as reported by Tredoux et al. (1989) and in Table 1. The PGE total content of samples characterized by enrichment in trevorite vary from 6196 to 7692 ppb, whereas in those

Always consult and cite the final, published document. See http://www.minsocam.org or GeoscienceWorld

characterized by the presence of abundant hydrous silicates the maximum concentration of PGE is 1012 ppb. Despite of the difference in the total PGE amount, all the analyzed samples are relatively depleted in IPGE (Os+Ir+Ru) especially in Os and Ir (Fig. 7). This is probably the explanation for why no Ir or Os species have been found. Among the PPGE (Rh+Pt+Pd), although Rh shows enriched chondrite normalized values, it must be borne in mind that Rh, in absolute terms, is by far the rarest of the PGE, which would explain why no Rh phases were found either.

The identification of native Ru associated with minerals of the Ni-Sb-As system (Fig. 1) does not account for reported whole-rock PGE abundance. Failure in finding a PGM assemblage consistent with geochemical data was probably caused by the uneven distribution of the PGM grains throughout the sample, which has as a consequence the fact that there is little chance to detect them in polished sections. Application of the hydroseparation technique has proved that the PGM are relatively abundant and include specific minerals of all the PGE, except Rh, Os and Ir. Furthermore, the occurrence of electrum accounts for the relatively high Au content in bulk rock amounting up to more than 300 ppb in samples of the trevorite-rich assemblage from the undeformed core of the body (Tredoux et al. 1989).

Origin of the PGM-Au assemblage

We note that the minute PGM and associated Ni-Fe-Sb-As inclusions in trevorite are not associated with fissures, fractures or crystal faces of the spinel phase. They rather appear as tiny, solid drops incorporated in trevorite, analogous to the primary magmatic PGM inclusions captured by chrome spinels crystallizing from mafic melts. Trevorite is known to be part of the secondary mineral assemblage together with nepouite and possibly formed during the main serpentinization event, coincident with exposure of the Bon Accord Ni-oxide body to near-surface hydrothermal conditions, but predating the last stage of schistosity (Tredoux et al. 1989). In this view, we can assume that all the PGM inclusions (Pd-Sb, Pd-Cu-Sb, Pd-Sb-As, Ru-S, and Pt-As-S) and the other Ni-Fe-Sb-As compounds, were present in the system at the time of trevorite crystallization. Their composition, comprising metal compounds of Sb and As, and above all their morphology and textural relationships do not support that these grains are remnants of primary minerals incorporated in secondary Ni oxide. More likely they precipitated in equilibrium with the hydrothermal conditions that generated the trevorite-nepouite secondary

Always consult and cite the final, published document. See http://www.minsocam.org or GeoscienceWorld

assemblage.

The origin of the PGM and electrum encountered in the concentrates as free grains is more difficult to be interpreted given the lack of any textural evidence. If the free grains of PGM and electrum are remnants of primary phases, then their paragenetic assemblage should fit one of the models proposed for the origin of the Bon Accord Ni-oxide body, and critically overviewed in Tredoux et al. (1989).

An extraterrestrial origin has been discarded based on many geochemical inconsistencies, including siderophile element ratios, and more recently by Cr isotopic data (Tredoux et al. 2013). An impact hypothesis may find some support in the recent discovery of nano-particles of PGE included in chondritic microspherules from deep-sea sediments of the Indian Ocean (Rudraswami et al. 2011) and the Paraburdoo-Reivilo Archaen layers of Western Australia and South Africa (Goderis et al. 2013). However, the markedly negative slope of the PGE chondritic patterns (high IPGE/PPGE ratio) with over-chondrite Ir and Os contents in the Indian Ocean micronuggets (Rudraswami et al. 2011), as well as the Rh-Pt-Pd-Au negative segment in the Archaen-layers microspherules (Goderis et al. 2013) are at odds with the Bon Accord occurrence (Fig. 7), as it is the systematic absence of Au phases in these astrobleme materials.

The PGM-Au mineral assemblage of Bon Accord neither supports a derivation from ophiolite-plutonic rocks (strongly residual mantle or podiform chromitites) in which IPGE predominate, and PPGE fractionation is strictly related with the presence of sulfides of magmatic or hydrothermal origin (Naldrett and Von Gruenewaldt 1989). The PGE chondrite-normalized patterns may recall those of several Ni-sulfide ores associated with mafic-ultramafic rocks. In particular, PGM members of the sobolevskite-kotulskite series and/or the uncommon association gold-sperrylite have been previously described from Norilsk (Evstigneeva and Kovalenker 1975), Talnotry (Power et al. 2004), Sudbury (Ames et al. 2007), and the Ivrea Zone (Garuti and Rinaldi 1986; Zaccarini et al. 2014). A number of Pt-Pd-Sb-As-Bi-Te PGM have been reported from nicheliferous sulfide deposits associated with komatiite such as Kambalda (Hudson 1986; Godel et al. 2012) and even from the low-sulfide PGE mineralization of Kevitsa (Kaukonen 2010) and Lukkulaisvaara (Groshovskaya et al. 1992). If the free-grains of PGM and electrum are remnants of a primary assemblage, Bon Accord might be the strongly metamorphosed equivalent of a small, low-sulfide mineralization enriched in PGE and Au. However, this model is undermined by several field and geochemical contrary evidences (Tredoux et al. 1989).

Always consult and cite the final, published document. See http://www.minsocam.org or GeoscienceWorld

Finally, the PGM mineralogy of Bon Accord has some features in common with micronuggets encountered in orogenic lherzolite possibly exhumed from sub-continental environments (Garuti et al. 1984; Lorand et al. 2010). The PGE distribution is rather unfractionated (low Pd/Ir ratio) with some Pd-Au enrichment in mantle massifs associated with deep granulitic crust (i.e. Ronda and Ivrea Zone, Crocket 2002). The PGM assemblage appears to be partly residual (Pt-Ir-Os alloys) having survived partial melting, and partly metasomatic (IPGE-Sb-Bi-Te compounds) being a result of mantle refertilization by reaction with percolating basaltic melts, or reworking under low-temperature hydrothermal conditions. However, mantle lherzolite, because of their fertile character, do not display the over-abundance of Ni observed in the Bon Accord samples that would be more consistent with material proceeding from the deep-mantle/core transition or the core itself.

As an alternative, we may speculate that the most likely textural position of the PGM and electrum, before liberation, was inside the nepouite matrix, together with the abundant Ni-As and Ni-Sb compounds described from Bon Accord (Tredoux et al. 2014, submitted). In this case, the entire mineral assemblage may have a common secondary origin, having been formed during the hydrothermal reworking of the Bon Accord Ni-oxide body. In a number of natural occurrences, precipitation of PGE-Sb-As-Bi-Te compounds together with PGE alloys, PGE oxides, may results from the low-sulfidation regime that usually accompanies hydrothermally driven serpentinization of mafic-ultramafic bodies.

The ligands in the newly formed PGM (As, Sb, Bi, Te, O) may be already present in the primary system but, more frequently, they proceed from the same source of the hydrothermal solutions. This has been reported from young and ancient ophiolite complexes and layered intrusions elsewhere in the world (Garuti and Zaccarini 1997; Zaccarini et al. 2005; 2006; Garuti et al. 2007; 2012; Tsoupas and Economou-Eliopoulos 2008; Proenza et al. 2008). In this model, the metals Ni-PGE-Au were original components of the primary mineral assemblage of the Bon Accord precursor, whereas As, Sb, Bi, Te, O might have been contributed by the metasomatizing fluids, during near-surface evolution of the ore body.

IMPLICATIONS

A major implication of this study is that the mineralogical investigation of very small and

Always consult and cite the final, published document. See http://www.minsocam.org or GeoscienceWorld

dispersed phases, like PGM, needs to combine different techniques. This is particularly required when results of simple *in situ* mineralogical analyses do not predict bulk-rock PGE contents in a sample. Our *in situ* mineralogical study on polished sections provides satisfactory data on the distribution and composition of very small PGM grains included in larger mineral host. However, interception of rare, large grains in polished sections has an unlikely chance of success. Therefore, large PGM may be poorly represented, although accounting for a big proportion of the total PGE amount in the sample. Mineralogical analyses based on separation of PGM from the matrix are unable to efficiently concentrate phases less than 5 micrometers in size, but allow treatment of a larger volume of samples, thus improving the possibility to encounter dispersed phases (Cabri et al. 2005a;b; Grammatikopoulos et al. 2007; Rudashevsky et al. 2002; 2004; Oberthür et al. 2008; Cabri 2012). As a consequence, the hydrosepration is a key technique enabling the study of very small and dispersed minerals. Therefore, the PGM should be investigated using both these complementary analytical methodologies to achieve more reliable and complete results.

In conclusion, the study of heavy-mineral concentrates from the Bon Accord Ni-oxide body has shown the existence of a complex PGM-Au mineral assemblage. The mineralogy is in good agreement with results of the PGE and Au analysis. There is convincing evidence that the PGM-Au minerals are of secondary origin, probably generated during low-temperature metamorphism of the ore body. The results of this study, although not conclusive, have contributed to cover an important lack of knowledge about the mineral residence of Pd, Pt, and Au in the Bon Accord Ni-oxide body.

ACKNOWLEDGMENTS

Justine Magson of the Geology Department of the University of the Free State is thanked for crushing and sieving the sample in preparation for hydroseparation. The University Centrum of Applied Geosciences of Austria (UCAG) is acknowledged for making available the facilities of the Eugen F. Stumpfl Microprobe Laboratory. Keith D. Putirka and Alejandro Fernandez-Martinez are gratefully thanked for their editorial review. This manuscript benefited from the constructive comments of Louis J. Cabri and Nigel Cook. Their very useful suggestions greatly improved the scientific quality of this manuscript.

REFERENCES

Ames, D.E., McClenaghan, M., and Averill, S. (2007) Footwall hosted Cu-PGE (Au, Ag), Sudbury Canada: Towards a new exploration vector. In "Proceedings of Exploration 07: Fifth Decennial International Conference on

Always consult and cite the final, published document. See http://www.minsocam.org or GeoscienceWorld

Mineral Exploration" (Ed. B. Milkereit), 1013-1017.

Barkov, A.Y., Martin, R.F., Halkoaho, T.A.A., and Criddle, A.J. (2002a) Laflammeite, $Pd_3Pb_2S_2$, a new platinum-group mineral species from the Penikat layered complex, Finland. The Canadian Mineralogist, 40, 671-678.

Barkov, A.Y., Martin, R.F., Pakhomovsky, Y.A., Tolstykh, N.D., and Krivenko, A.P. (2002b) Menshikovite, $Pd_3Ni_2As_3$, a new platinum-group mineral species from two layered complexes, Russia. The Canadian Mineralogist, 40, 679-692.

Botelho, N.F, Moura, M.A., Stanley, C.J., and Silva, D.V.G. (2006) Kalungaite, PdAsSe, a new platinum-group mineral from the Buraco do Ouro gold mine, Cavalcante, Goiás State, Brazil. Mineralogical Magazine, 70, 123-130.

Cabri, L.J., Criddle, A.J., Laflamme, J.H.G., Bearne, G.S., and Harris, D.C. (1981) Mineralogical study of complex Pt-Fe nuggets from Ethiopia. Bulletin de Mineralogie, 104, 508-525.

Cabri, L.J. (2002) The platinum-group minerals. In The geology, geochemistry, mineralogy and mineral beneficiation of platinum-group elements (Ed. L.J. Cabri), Canadian Institute of Mining, metallurgy and petroleum, special volume, 54, 13-129.

Cabri, L.J., Beattie, M., Rudashevsky, N.S., and Rudashevsky, V.N. (2005a) Process mineralogy of Au, Pd and Pt ores from the Skaergaard intrusion, Greenland, using new technology. Minerals Engineering, 18, 887-897.

Cabri, L.J., McDonald, A.M., Stanley, C.J., Rudashevsky, N.S., Poirier, G., Durham, B.R., Mungall, J.E., and Rudashevsky, V.N. (2005b) Naldrettite, Pd_2Sb, a new intermetallic mineral from the Mesamax Northwest deposit, Ungava region, Quebec, Canada. Mineralogical Magazine, 69, 89-97.

Cabri, L.J. (2012) Comment on "Changes in sulfides and platinum-group minerals with the degree of alteration in the Roby, Twilight, and High Grade Zones of the Lac des Iles Complex, Ontario, Canada" by MLN Djon and SJ Barnes. Mineralium Deposita, 47, 949-952.

Coghill, B.M., and Wilson, A.H. (1993) Platinum-group minerals in the Selukwe Subchamber, Great Dyke, Zimbabwe: implications for PGE collection mechanisms and post-formational redistribution. Mineralogical Magazine, 57, 613-633.

Cook, N.J., Ciobanu, C.L. Merkle, R.K.W., and Bernhardt, H.J. (2002) Sobolevskite, taimyrite, and Pt_2CuFe (tulameenite) in complex massive Talnakhite ore, Norilsk orefield, Russia. The Canadian Mineralogist, 40, 329-340.

Always consult and cite the final, published document. See http://www.minsocam.org or GeoscienceWorld

Crocket J.H. (2002) Platinum-group element geochemistry of mafic and ultramafic rocks. In The geology, geochemistry, mineralogy and mineral beneficiation of platinum-group elements (Ed. L.J. Cabri), Canadian Institute of Mining, metallurgy and petroleum, special volume, 54, 177-210.

Daltry, V.D.C., and Wilson, A.H. (1997) Review of platinum-group mineralogy: compositions and elemental associations of the PG-minerals and unidentified PGE- phases. Mineralogy and Petrology, 60, 185-2.

De Waal, S.A. (1972) Nickel minerals from Barberton, South Africa: IV: Ferroan trevorite, redescribed. American Mineralogist, 57, 1524-1527.

De Waal, S.A., and Calk, L.C. (1973) Nickel minerals from Barberton, South Africa: VI: Liebenbergite, a nickel olivine. American Mineralogist, 58, 733-735.

De Waal, S.A. (1978) The nickel deposit at Bon Accord, Barberton, South Africa – A proposed paleometeorite. In Mineralisation in metamorphic terranes (ed. W.J. Verwoerd), Geological Society of South Africa, Johannesburg, 87-98.

De Waal, S.A. (1979) The metamorphism of the Bon Accord nickel deposit by the Nelspruit granite. Transactions of the Geological Society of South Africa, 82, 335-342.

De Wit M.J., Hart R.A., and Hart R.J. (1987). The Jamestown ophiolite complex, Barberton Mountain Land: A composite section through 3.5 Ga simatic lithosphere. Journal of African Earth Sciences, 6, 681-730.

Evstigneeva, T.L., and Kovalenker, V.A. (1975) Sobolevskite, a new bismuthide of palladium and the nomenclature of minerals of the system PdBi-PdTe-PdSb. International Geology Review, 18, 856-866.

Garuti, G., Gorgoni, C., and Sighinolfi, G.P. (1984) Sulfide mineralogy and chalcophile and siderophile element abundances in the Ivrea-Verbano mantle peridotites (Western Italian Alps). Earth and Planetary Science Letters, 70, 69-87.

Garuti, G., and Rinaldi, R. (1986) Mineralogy of melonite-group and other tellurides from the Ivrea-Verbano basic complex, Western Italian Alps. Economic Geology, 81, 1213-1217.

Garuti G., and Zaccarini, F. (1997) In situ alteration of platinum-group minerals at low temperature: evidence from serpentinized and weathered chromitite of the Vourinos Complex, Greece. The Canadian Mineralogist, 35, 611-626.

Garuti, G., Zaccarini F., Cabella, R., and Fershtater, G. (1997) Occurrence of unknown Ru- Os-Ir-Fe oxides in the

Always consult and cite the final, published document. See http://www.minsocam.org or GeoscienceWorld

418 chromitites of the Nurali ultramafic complex, southern Urals, Russia. The Canadian Mineralogist, 35, 1431-1440.
419
420 Garuti, G., Proenza, J.A., and Zaccarini, F. (2007): Distribution and mineralogy of platinum-group elements in
421 altered chromitites of the Campo Formoso layered intrusion (Bahia State, Brazil): control by magmatic and
422 hydrothermal processes. Mineralogy and Petrology, 86, 159-188.
423
424 Garuti, G., Zaccarini, F., Proenza, J.A., Thalhammer, O.A.R., and Angeli, N. (2012) Platinum-group minerals in
425 chromitites of the Niquelândia layered intrusion (Central Goias, Brazil): Their magmatic origin and low-temperature
426 reworking during serpentinization and lateritic weathering. Minerals, 2, 365-384.
427
428 Godel, B., Gonzales-Alvarez, I., Barnes, S.J., Barnes S.-J., Parker, P., and Day, J. (2012) Sulfides and sulfarsenides
429 from the Rosie Nickel Prospect, Duketon greenstone belt, Western Australia. Economic Geology, 107, 275-294.
430
431 Goderis, S., Simonson, B.M., McDonald, I., Hassler, S.W., Izmer, A., Belza, A., Terryn, H., Vanhaecke, F., and
432 Claeys, P. (2013) Ni-rich spinels and platinum group element nuggets condensed from a Late Archean impact
433 vapour cloud. Earth and Planetary Science Letters, 376, 87-98.
434
435 Grammatikopoulos, T., Kapsiotis, A., Zaccarini, F., Tsikouras, B., Hatzipanagiotou, K., and Garuti, G. (2007)
436 Platinum group mineral characterization in concentrates from chromitites, Pindos ophiolite complex, northern
437 Greece. Minerals Engineering, 20, 1170-1178.
438
439 Groshovskaya, T.L., Distler, V.V., Klyunin, S.F., Zakharov, A.A., and Laputina, I.P. (1992) Low-sulfide platinum
440 group mineralization of the Lukkulaisvaara pluton, northern Karelia. International Geology Review, 34, 503-520.
441
442 Jedwab, J., and Cassedanne, J. (1998) Historical observations on oxygen-bearing compounds of platinum and
443 palladium in Minas Gerais, Brazil. The Canadian Mineralogist, 36, 887-893.
444
445 Hudson, D.R. (1986) Platinum-group minerals from the Kambalda Nickel deposits, Western Australia. Economic
446 Geology, 81, 1218-1225.
447
448 Kapsiotis, A., Grammatikopoulos, T., Tsikouras, B., Hatzipanagiotou, K., Zaccarini, F., and Garuti, G. (2009)
449 Chromian spinel composition and platinum group elements mineralogy of chromitites from the Milia Area, Pindos
450 ophiolite complex, Greece. The Canadian Mineralogist, 47, 1037-1056.
451
452 Kaukonen, R. (2010) Advanced and sustainable beneficiation of platinum-group minerals in sulfide-poor platinum
453 deposits – BEPGE Mineralogy subproject. Final report. Res Terrae, 20, 5-31.
454

Always consult and cite the final, published document. See http://www.minsocam.org or GeoscienceWorld

Kojonen, K.K., Tarkian, M., Roberts, A.C., Törnroos, R., and Heidrich, S. (2007) Miessiite, $Pd_{11}Te_2Se_2$, a new mineral species from Miessijoki, Finnish Lapland, Finland. The Canadian Mineralogist, 45, 1221-1227.

Kovalenker, V.A., Genkin, A.D., Estigneeva, T.L., and Laputina, I.P. (1975) Telarpagite, a new mineral of palladium, silver and tellurium from the copper-nickel ores of the Oktyabr deposit. International Geology Review, 17, 817-822.

Lorand, J.-P., Alard, O., and Luguet, A. (2010) Platinum-group element micronuggets and refertilization processes in Lherz orogenic peridotite (northeastern Pyrenees, France). Earth and Planetary Science Letters, 289, 298-310.

McDonald, A.M., Cabri, L.J., Stanley, C.J., Rudashevsky, N.S., Poirier, G., Mungall, J.E., Ross, K.C., Durham, B.R., and Rudashevsky, V.N. (2005) Ungavaite, Pd4Sb3, a new intermetallic mineral species from the Mesamax northwest deposit, Ungava Region, Quebec, Canada: description and genetic implications. The Canadian Mineralogist, 43, 1735-1744.

McDonald, A.M., Proenza, J., Zaccarini, F., Rudashevsky, N., Cabri, L.J., Stanley, C.J., Rudashevsky, V., Melgarejo, J.C., Lewis, J., Longo, F., and Bakker, R.J. (2010) Garutiite, (Ni, Fe, Ir) a new hexagonal form of native Ni from Loma Peguera, Dominican Republic. European Journal of Mineralogy, 22, 293-304.

McDonald, I., Ohnenstetter, D., Rowe, J.P., Tredoux, M., Pattrick, R.A.D., and Vaughan, D.J. (1999) Platinum precipitation in the Waterberg deposit, Naboomspruit, South Africa. South African Journal of Geology, 102, 184-191.

Mochalov, A.G., Tolkachev, M.D., Polekhovsky, Yu.S., and Goryacheva E.M. (2007) Bortnikovite, Pd_4Cu_3Zn, a new mineral species from the unique Konder placer deposit, Khabarovsk krai, Russia. Geology of Ore Deposits, 49, 318-327.

Naldrett, A.J., and Duke, J.M. (1980) Platinum metals in magmatic sulfide ores. Science 208, 1417-1424.

Naldrett, A.J., and Von Gruenewaldt, G. (1989): Association of Platinum-Group Elements with chromitite in layered intrusions and ophiolite complexes. Economic Geology. 84, 180-187.

Oberthür, T., Melcher, F., Sitnikova, M., Rudashevsky, N.S., Rudashevsky, V.N., Cabri, L.J., Lodziak, J., Klosa, D., and Gast, L. (2008): Combination of novel mineralogical methods in the study of noble metal ores - Focus on pristine (Bushveld, Great Dyke) and placer platinum mineralisation. The Australasian Institute of Mining and Metallurgy, 8, 187-194.

Always consult and cite the final, published document. See http://www.minsocam.org or GeoscienceWorld

Paar, W.H., Topa, D., Makovicky, E., Sureda, R.J., de Brodtkorb, M.K., Nickel, E.H., and Putz, H. (2004) Jagueite, $Cu_2Pd_3Se_4$, a new mineral species from EL Chire, La Rioja, Argentina. The Canadian Mineralogist 42, 1745-1755.

Paar, W.H., Topa, D., Makovicky, E., and Culetto F.J. (2005) Milotaite, PdSbSe, a new palladium mineral species from Redb Rice, Czech Republic. The Canadian Mineralogist 43, 689-694.

Partridge, F.C. (1944) Trevorite and a suggested new nickel-bearing silicate from Bon Accord, Sheba Siding, Barberton district. Transactions of the Geological Society of South Africa, 46, 119-126.

Power, M.R., Pirrie, D., Jedwab, J., and Stanley, C.J. (2004) Platinum-group element mineralization in an As-rich magmatic sulphide system, Talnotry, southwest Scotland. Mineralogical Magazine, 68, 395-411.

Proenza, J.A., Zaccarini, F., Escayola, M., Cábana, C., Schalamuk, A., and Garuti, G., (2008) Composition and textures of chromite and platinum-group minerals in chromitites of the western ophiolitic belt from Pampeans Ranges of Córdoba, Argentina. Ore Geology Review, 33, 32-48.

Rudashevsky, N.S., Garuti, G., Andersen, J.C.Ø., Kretser, Y.L., Rudashevsky, V.N., and Zaccarini, F. (2002) Separation of accessory minerals from rocks and ores by hydroseparation (HS) technology: method and application to CHR-2 chromitite, Niquelandia, Brazil. Applied Earth Sciences (Transaction of the Institution of Mining and Metallurgy, section B) 111, B87-B94.

Rudashevsky, N.S., McDonald, A.M., Cabri, L.J., Nielsen, T.D.F., Stanley, C.J., Kretzer, Yu. L., and Rudashevsky, V.N. (2004) Skaergaardite, PdCu, a new platinum-group intermetallic mineral from the Skaergaard intrusion, Greenland. Mineralogical Magazine 68, 603-620.

Rudraswami, N.G., Parashar, K., and Shyam Prasad, M. (2011) Micrometer- and nanometer-sized platinum group nuggets in micrometeorites from deep-sea sediments of the Indian Ocean. Meteoritics & Planetary Science, 46, 470-491.

Shi, C.Y., Zhang, L., Yang, W., Lui, Y., Wang, J., Meng, Y., Andrews, J.C., and Mao, W.L. (2013) Formation of an interconnected network of iron melt at Earth's lower mantle conditions. Nature Geoscience, 6, 971-975.

Stanley, C.J., Criddle, A.J., Forster, H.J., and Roberts, A.C., (2002) Tischendorfite, $Pd_8Hg_3Se_9$, a new mineral species from Tilkerode, Harz Mountains, Germany. The Canadian Mineralogist, 40, 739-745.

Tredoux, M., de Wit, M.J., Hart, R.J., Armstrong, R.A., Lindsay, N.M., and Sellschop, J.P.F. (1989) Platinum group elements in a 3.5 Ga nickel-iron occurrence, possible evidence of a deep mantle origin. Journal of Geophysical

Always consult and cite the final, published document. See http://www.minsocam.org or GeoscienceWorld

529 Research, 94(B1), 795-813.
530
531 Tredoux, M., Roelofse, F., and Shukolyukov, A. (2013) Isotope characteristics of the Bon Accord oxide body,
532 Barberton greenstone belt, South Africa. Mineralogical Magazine, 77, 2371.
533
534 Tredoux, M., Zaccarini, F., Garuti, G., and Miller, D. E. (2014) An investigation of phases in the Ni-Sb-As system,
535 and associated platinum-group minerals, which occur in the Bon Accord oxide body, Barberton greenstone belt,
536 South Africa. Mineralogical Magazine, submitted.
537
538 Trevor, T.G. (1920) Nickel: Notes on the occurrence in the Barberton district. South African Journal of Industry, 3,
539 532-533.
540
541 Tsoupas, G., and Economou-Eliopoulos, M. (2008). High PGE contents and extremely abundant PGE-minerals
542 hosted in chromitites from the Veria ophiolite complex, northern Greece. Ore Geology Reviews 33, 3-19.
543
544 Uysal, I., Zaccarini, F., Sadiklar, M.B., Bernhardt, H.J., M., Bigi, S., and Garuti, G. (2009) Occurrence of rare Ru-
545 Fe-Os-Ir-oxide and associated Platinum-group minerals (PGM) in the chromitite of Mugla ophiolite, SW-Turkey.
546 Neues Jahrbuch fur Mineralogie Abhandlungen, 185, 323-333.
547
548 Vymazalova, A., Laufek, F., Drabek, M., Haloda, J., Sidorinova, T., and Plasil, J. (2009): Pasavaite, $Pd_3Pb_2Te_2$, a
549 new platinum-group mineral species from Noril`sk-Talnakh Ni-Cu camp, Russia. Canadian Mineralogist 47, 1, 53-
550 62.
551
552 Vymazalova, A., Laufek, F., Drabek, M, Cabral, A.R., Haloda, J., Sidorinov, T., Lehmnn, B., Galbiatti, H.F., and
553 Drahokoupil, J. (2012a) Jacutingaite, Pt_2HgSe_3, a new platinum-group mineral from the Cauê iron-ore deposit,
554 Itabira District, Minas Gerais, Brazil. The Canadian Mineralogist 50, 431-440.
555
556 Vymazalova, A., Laufek, F., Drabek, M., Stanley, C.J., Baker, R.J., Bermejo, R., Garuti, G., Thalhammer, O.,
557 Proenza, J.A., and Longo, F. (2012b) Zaccariniite, RhNiAs, a new platinum-group minera species from Loma
558 Peguera, Dominican Republic. The Canadian Mineralogist, 50, 1321-1329.
559
560 Vymazalova, A., Drabek, M., Zaccarini, F., Garuti, G., and Evstigneeva, T. (2013) Kotulskite-sobolevskite solid
561 solution, natural occurrence and an experimental investigation. In "Mineral deposit research for a high-tech world"
562 edited by E. Jonsson et al., Proceedings of the 12th Biennal SGA meeting, 383-386.
563
564 Walker, T. L. (1923) Trevorite a distinct mineral species. University of Toronto Studies, 16, 53.
565

Always consult and cite the final, published document. See http://www.minsocam.org or GeoscienceWorld

Watkinson, D.H., and Ohnenstetter, D. (1992) Hydrothermal origin of platinum-group mineralization in the Two Duck Lake intrusion, Coldwell complex, northwestern Ontario. The Canadian Mineralogist, 30, 121-136.

Yu, Z., Cheng, F., and Ma, H. (2009) Lisiguangite, $CuPtBiS_3$, a new platinum-group mineral from the Yanshan Mountains, Hebei, China. Acta Geologica Sinica, 83, 238-244.

Zaccarini, F., Proenza, J.A., Ortega-Gutierrez F., and Garuti, G. (2005) Platinum Group Minerals in ophiolitic chromitites from Tehuitzingo (Acatlan Complex, Southern Mexico): implications for postmagmatic modification. Mineralogy and Petrology, 84, 147-168.

Zaccarini, F., Garuti, G., and Martin, R.F. (2006) Exotic accessory minerals in layered chromitites of the Campo Formoso complex (Brazil). Geologica Acta, 4, 461-469.

Zaccarini, F., Garuti, G., Fiorentini, M.L., Locmelis, M., Kolleger, P., and Thalhammer, O.A.R. (2014) Mineralogical host of plarinum group elements (PGE) and rhenium in the magmatic Ni-Fe-Cu sulfide deposits of the Ivrea Verbano Zone (Italy): An electron microprobe study. Neues Jahrbuch für Mineralogie Abhandlugen, 191, 169-187.

Zaccarini, F., Proenza, J., Rudashevsky, N., Cabri, L. J., Garuti, G., Rudashevsky, V., Melgarejo, J.C., Lewis, J., Longo, F., Bakker, R.J., and Stanley, C. (2009) The Loma Peguera ophiolitic chromitite (Central Dominican Republic): a source of new platinum group minerals (PGM) species. Neues Jahrbuch für Mineralogie Abhandlungen, 185, 334-349.

Captions to figures.

FIGURE 1. BSE image of ruthenium associated with a $Ni_7(As,Sb)$, trevorite and cloroapatite and included in a Ni-rich silicate, found during the *in situ* investigation of Bon Accord polished and thin sections.

FIGURE 2. FE-SEM images of poly-phase PGM and Fe-Ni-As phase included in trevorite, found in the concentrates of Bon Accord. A = large view. B = bi-phase grain composed of a Pd-Sb-As and Pd-Sb compounds. C = = bi-phase grain composed of a Pd-Cu-Sb and Pd-Sb. D, E =

Always consult and cite the final, published document. See http://www.minsocam.org or GeoscienceWorld

601 complex PGM of Ru-S, Fe-Ni-Sb and Pt-Sb. F = single phase of Fe-Ni-As.
602
603 **FIGURE 3**. FE-SEM images of single phase PGM found in the concentrates. A = Ru-S
604 compound. B, C and D = grains composed of Pd-Sb.
605
606 **FIGURE 4**. FE-SEM images of free PGM and gold found in the heavy mineral concentrates of
607 Bon Accord. A, B and C = sperrylite single phase. D = Electrum single phase. E = Bi-phase
608 grain composed of sperrylite and electrum. F = enlargement of the grain shown in E.
609
610 **FIGURE 5**. BSE images of free grains of sobolevskite (A, B) and a Pd-Te-Bi compound (C)
611 found in the Bon Accord heavy mineral concentrate.
612
613 **FIGURE 6.** Composition (At%) of PGM from Bon Accord (black square) plotted in the Pd-Bi-Sb
614 ternary diagram, compared with that from other localities. Grey circle = Norilsk (Kovalenker et
615 al. 1975; Evstigneva and Kovalenker 1976), white circle = Lukkulaisvaara (Groshovskaya et al.
616 1992), black circle = Two Duck Lake (Watkinson and Ohnenstetter 1992), grey square = Great
617 Dyke (Coghill and Wilson 1993). Compositional fields after Cook et al. (2002).
618
619 **FIGURE 7.** PGE and Au chondrite-normalized (Naldrett and Duke 1980) patterns of the Bon
620 Accord samples (data from Tredoux et al. 1989).
621
622

Always consult and cite the final, published document. See http://www.minsocam.org or GeoscienceWorld

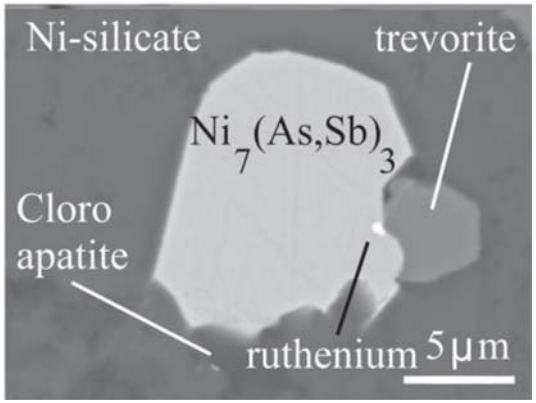
Ni-silicate
trevorite
$Ni_7(As,Sb)_3$
Cloro
apatite
ruthenium
5 µm

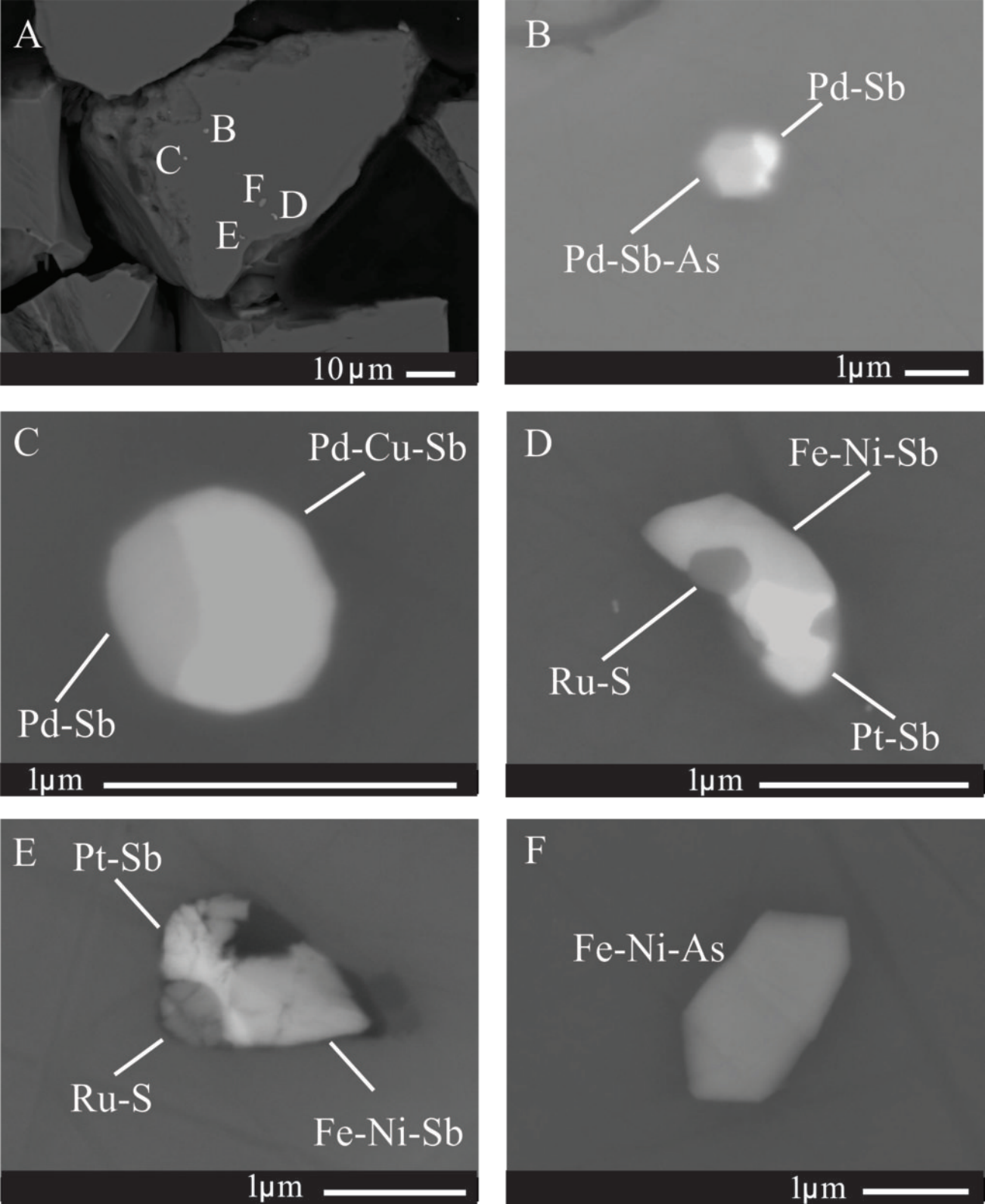
A
B
C
F
D
E
10 µm
B
Pd-Sb
Pd-Sb-As
1µm
C
Pd-Cu-Sb
Pd-Sb
1µm
D
Fe-Ni-Sb
Ru-S
Pt-Sb
1µm
E
Pt-Sb
Ru-S
Fe-Ni-Sb
1µm
F
Fe-Ni-As
1µm

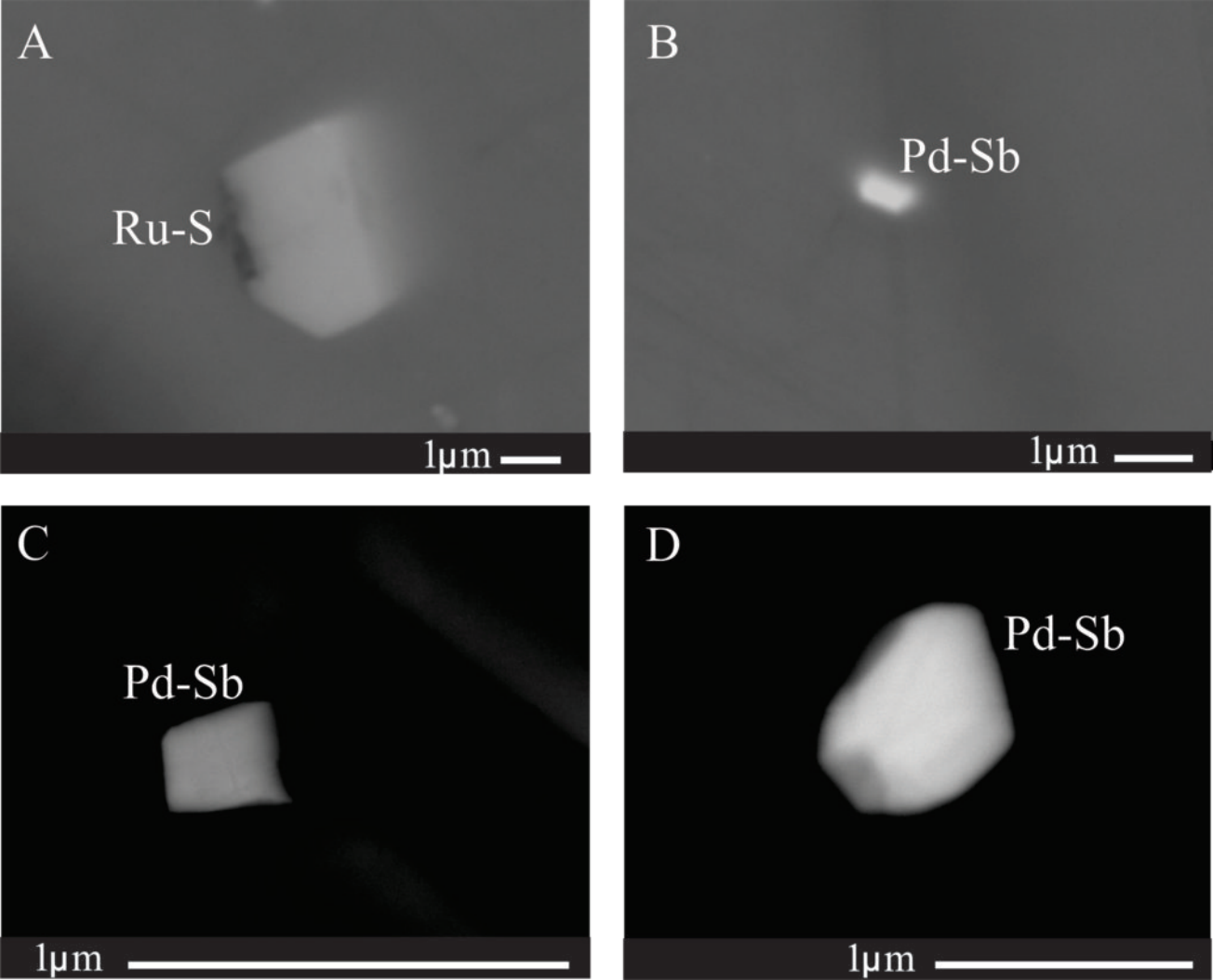
A
Ru-S
1μm
B
Pd-Sb
1μm
C
Pd-Sb
1μm
D
Pd-Sb
1μm

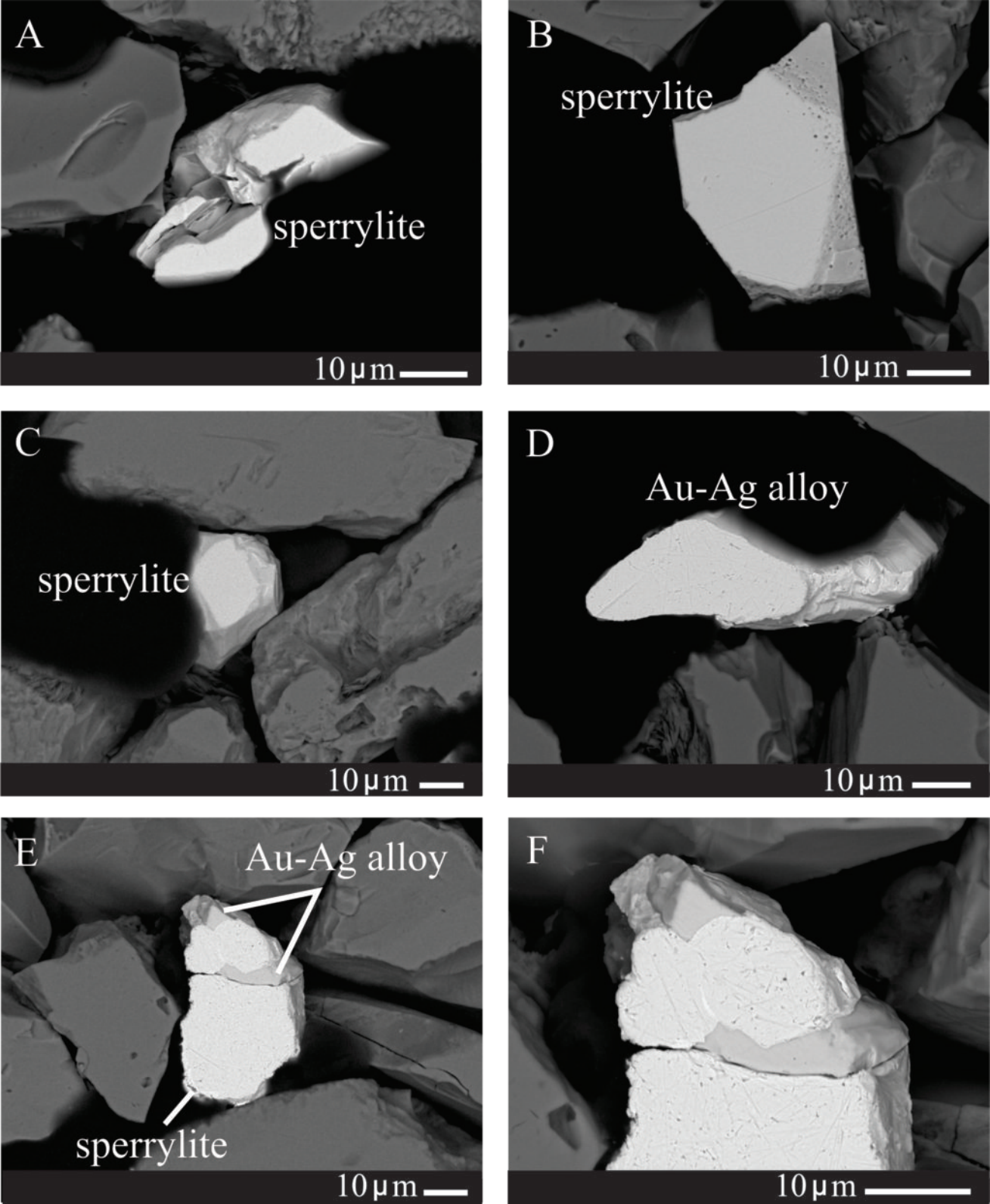
A
sperrylite
10 µm
B
sperrylite
10 µm
C
sperrylite
10 µm
D
Au-Ag alloy
10 µm
E
Au-Ag alloy
sperrylite
10 µm
F
10 µm

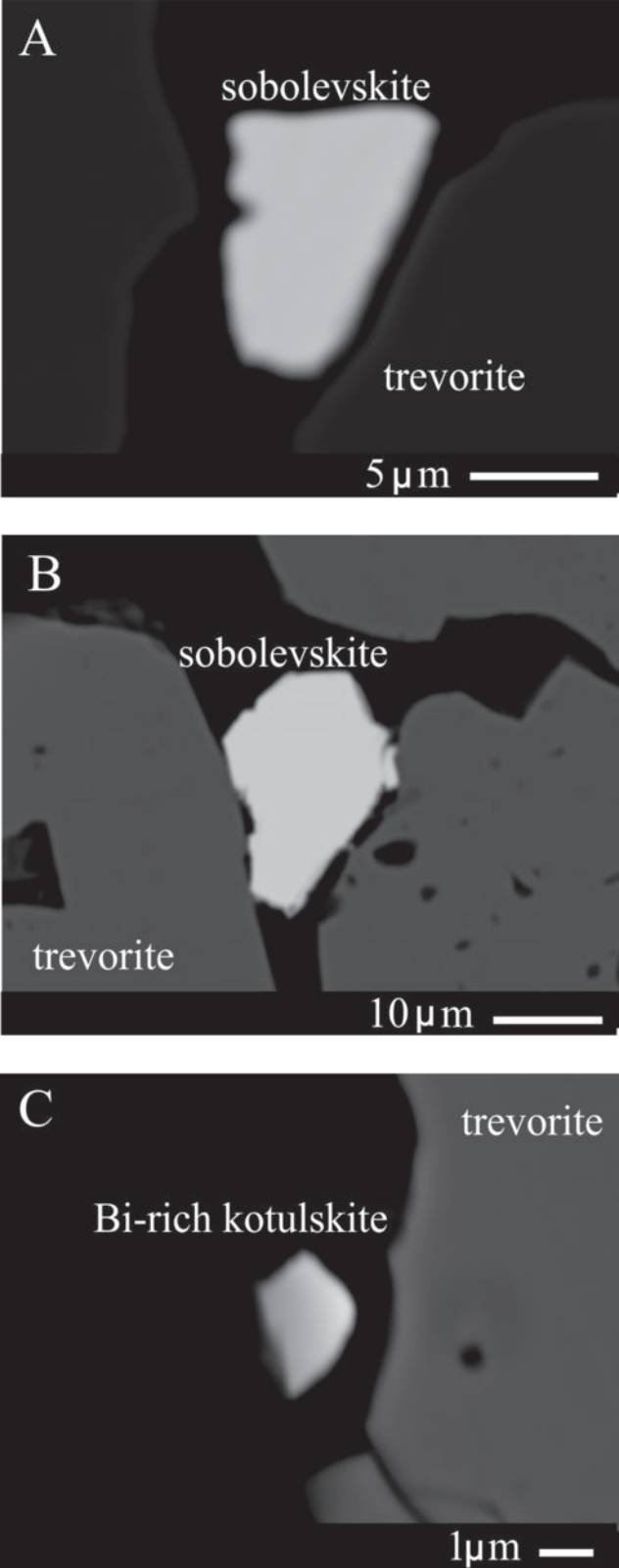
A
sobolevskite
trevorite
5 µm
B
sobolevskite
trevorite
10 µm
C
trevorite
Bi-rich kotulskite
1µm

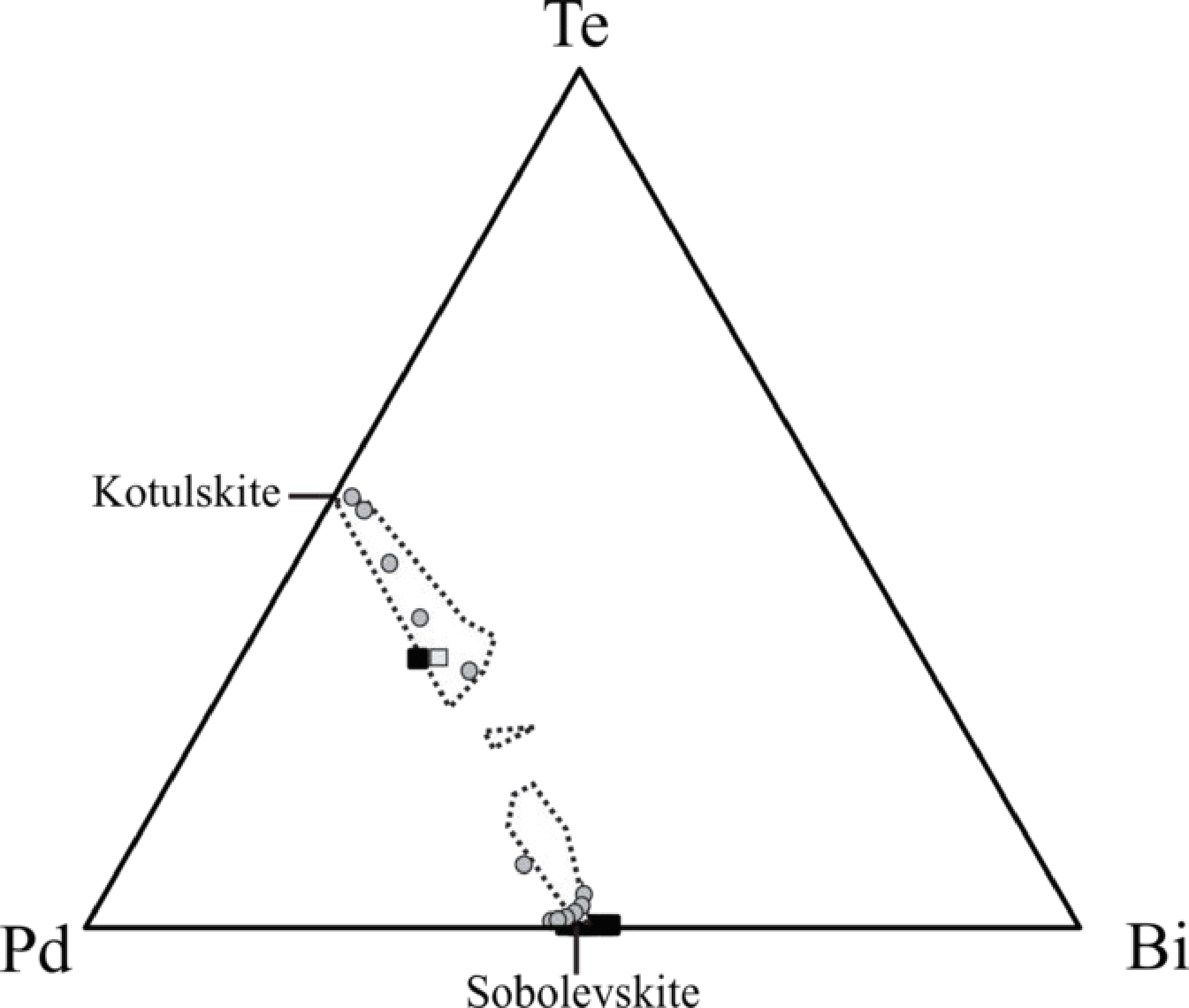
Te
Kotulskite
Pd
Bi
Sobolevskite

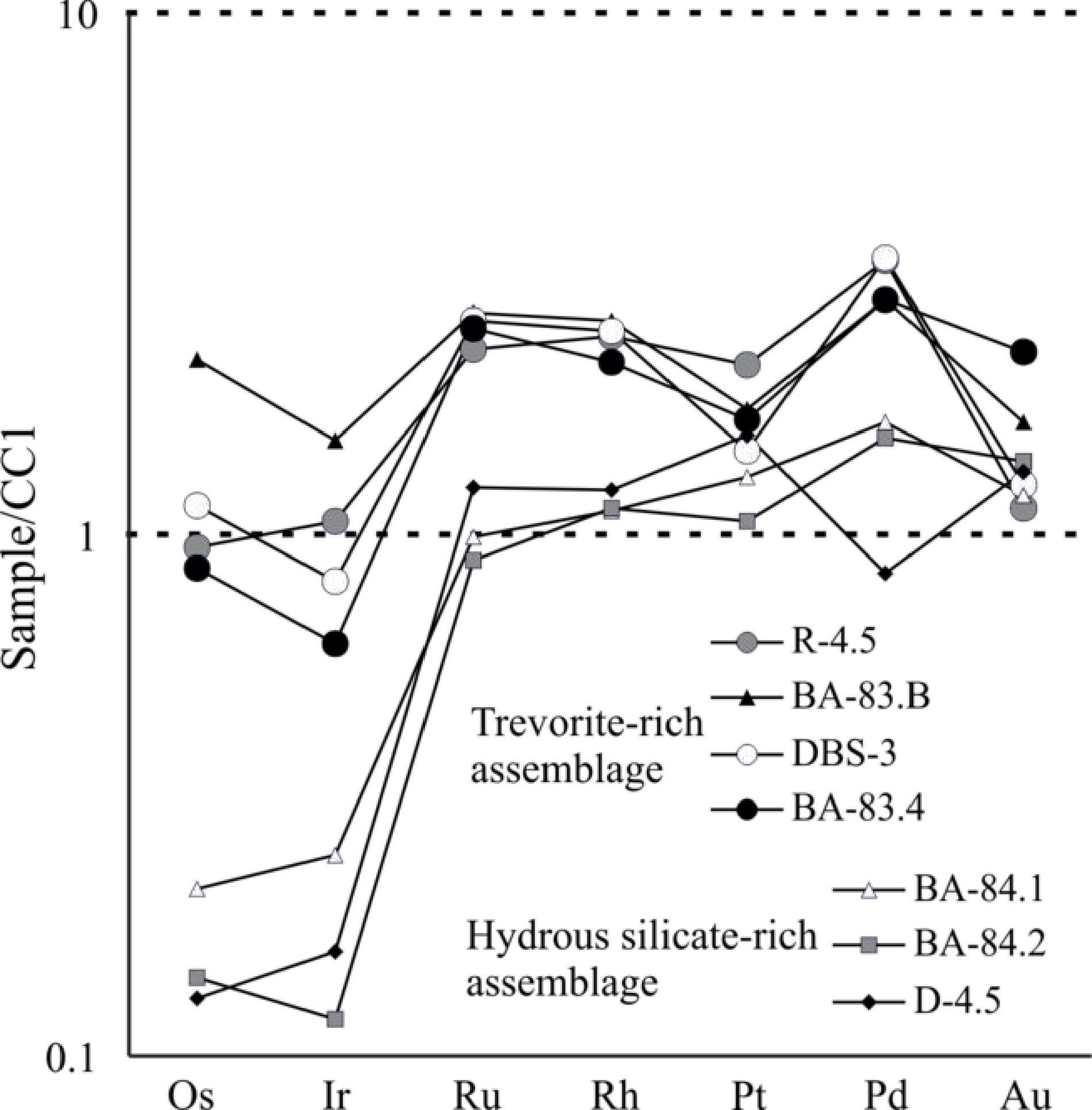
10
1
0.1
Sample/CC1
Os
Ir
Ru
Rh
Pt
Pd
Au
R-4.5
BA-83.B
DBS-3
BA-83.4
Trevorite-rich
assemblage
BA-84.1
BA-84.2
D-4.5
Hydrous silicate-rich
assemblage

TABLE 1. PGE and Au concentration (ppb) in selected samples of Bon Accord

	Os	Ir	Ru	Rh	Pt	Pd	Au	Total PGE
Trevorite-rich assemblage								
R-4.5	488	651	1556	478	2166	1825	170	7164
BA-83.B	1114	932	1830	515	1764	1537	250	7692
DBS-3	584	501	1771	493	1478	1845	190	6672
BA-83.4	441	380	1722	426	1694	1533	340	6196
Hydrous silicates-rich assemblage								
BA-84.1	108	150	684	221	1321	896	180	3380
BA-84.2	73	72	617	225	1078	833	210	2898
L-4.5	66	97	849	242	1583	461	200	3298

(data source: Tredoux et al. 1989)

TABLE 2. Selected electron microprobe analyses of electrum from Bon Accord

Wt%	Au	Ag	Fe	Ni	Cu	Bi	Te	S	Total
NCHminus53A-1	70.47	29.72	0.22	0.05	0.11	0.36	0.05	b.d.l.	100.97
NCHminus53A-2	72.34	27.73	0.26	0.04	0.18	0.47	0.04	b.d.l.	101.06
NCHminus53A-3	70.34	27.81	0.18	0.02	0.16	0.42	0.07	b.d.l.	99.01
NCHminus53A-4	70.63	28.90	0.23	0.04	0.17	0.35	0.07	0.05	100.43
NCHminus53A-5	70.07	28.72	0.31	0.04	0.18	0.40	0.04	0.07	99.82
NCHminus53A-6	71.55	28.36	0.31	0.04	0.17	0.39	0.07	0.03	100.92
NCHminus53A-7	70.54	29.11	0.35	0.04	0.17	0.38	0.08	0.04	100.72
NCHminus53A-8	68.85	27.31	0.58	0.08	0.15	0.43	0.06	0.04	97.51
NCHminus53A-9	71.70	27.95	0.22	0.03	0.11	0.37	0.07	0.02	100.47
NCHminus53A-10	70.60	28.65	0.71	0.09	0.15	0.28	0.06	0.02	100.56
NCHminus53A-11	70.83	28.20	0.36	0.04	0.14	0.30	0.06	0.01	99.93
NCHminus53A-12	72.46	27.31	0.30	0.03	0.14	0.46	0.06	0.02	100.78
NCHminus53A-13	69.63	27.99	0.18	0.03	0.17	0.35	0.07	b.d.l.	98.42
NCHminus53A-14	69.75	28.15	0.27	0.03	0.18	0.49	0.08	b.d.l.	98.95
NCHminus53A-15	70.12	26.64	0.25	0.06	0.19	0.47	0.07	0.03	97.83
NCHminus53A-16	70.03	28.03	0.46	0.08	0.14	0.44	0.06	0.03	99.27
NCHminus53A-17	70.20	27.08	0.30	0.05	0.18	0.44	0.07	0.05	98.38

At%	Au	Ag	Fe	Ni	Cu	Bi	Te	S	Total
NCHminus53A-1	55.78	42.90	0.61	0.12	0.26	0.27	0.06	b.d.l.	100
NCHminus53A-2	57.86	40.45	0.75	0.10	0.44	0.35	0.05	b.d.l.	100
NCHminus53A-3	57.29	41.30	0.52	0.05	0.41	0.33	0.09	b.d.l.	100
NCHminus53A-4	56.28	41.99	0.64	0.10	0.42	0.26	0.08	0.23	100
NCHminus53A-5	56.02	41.87	0.88	0.09	0.44	0.30	0.05	0.35	100
NCHminus53A-6	56.92	41.14	0.87	0.11	0.42	0.29	0.09	0.16	100
NCHminus53A-7	55.87	42.04	0.98	0.11	0.42	0.29	0.09	0.20	100
NCHminus53A-8	56.35	40.76	1.67	0.23	0.38	0.33	0.07	0.20	100
NCHminus53A-9	57.61	40.95	0.62	0.09	0.28	0.28	0.09	0.09	100
NCHminus53A-10	55.77	41.27	1.98	0.24	0.36	0.21	0.08	0.11	100
NCHminus53A-11	56.89	41.30	1.03	0.11	0.34	0.22	0.07	0.04	100
NCHminus53A-12	58.21	40.00	0.84	0.08	0.35	0.35	0.08	0.09	100
NCHminus53A-13	56.90	41.71	0.52	0.07	0.44	0.27	0.09	b.d.l.	100

NCHminus53A-14	56.57	41.63	0.78	0.08	0.46	0.37	0.10	b.d.l.	100
NCHminus53A-15	57.90	40.11	0.74	0.17	0.49	0.36	0.09	0.15	100
NCHminus53A-16	56.41	41.17	1.31	0.21	0.35	0.33	0.08	0.13	100
NCHminus53A-17	57.44	40.41	0.87	0.15	0.45	0.34	0.09	0.26	100

b.d.l. = below detection limit.

TABLE 3. Selected electron microprobe analyses of sperrylite from Bon Accord

Wt%	As	S	Os	Ir	Ru	Rh	Pt	Pd	Fe	Ni	Cu	Total
NCHminus53B-1a	42.99	0.80	0.43	0.16	0.39	0.77	53.07	0.18	1.27	0.16	b.d.l.	100.22
NCHminus53B-1b	41.93	0.86	0.64	0.14	0.36	0.85	53.59	b.d.l.	1.37	0.17	b.d.l.	99.90
NCHminus53B-2a	42.99	0.66	0.21	0.48	0.25	0.92	52.48	0.24	2.01	0.17	b.d.l.	100.41
NCHminus53B-3a*	43.75	0.49	b.d.l.	b.d.l.	b.d.l.	1.10	51.58	0.26	2.49	0.22	0.03	99.89
At%	As	S	Os	Ir	Ru	Rh	Pt	Pd	Fe	Ni	Cu	Total
NCHminus53B-1a	62.91	2.72	0.25	0.09	0.42	0.82	29.82	0.19	2.49	0.29	0.00	100
NCHminus53B-1b	61.87	2.97	0.37	0.08	0.39	0.92	30.37	0.02	2.71	0.31	0.00	100
NCHminus53B-2a	62.39	2.24	0.12	0.27	0.27	0.97	29.25	0.25	3.91	0.31	0.01	100
NCHminus53B-3a*	63.12	1.64	b.d.l.	b.d.l.	b.d.l.	1.15	28.58	0.26	4.81	0.40	0.05	100
apfu	As	S	Os	Ir	Ru	Rh	Pt	Pd	Fe	Ni	Cu	Total
NCHminus53B-1a	1.89	0.08	0.01	0.00	0.01	0.02	0.89	0.01	0.07	0.01	b.d.l.	3
NCHminus53B-1b	1.86	0.09	0.01	0.00	0.01	0.03	0.91	b.d.l.	0.08	0.01	b.d.l.	3
NCHminus53B-2a	1.87	0.07	0.00	0.01	0.01	0.03	0.88	0.01	0.12	0.01	b.d.l.	3
NCHminus53B-3a*	1.89	0.05	b.d.l.	b.d.l.	b.d.l.	0.03	0.86	0.01	0.14	0.01	0.00	3

n.a. = not analyzed, b.d.l. = below detection limit, * = intergrown with gold

TABLE 4. Selected electron microprobe analyses of sobolevskite and PdTeBi compound from Bon Accord

Wt%	Pd	Fe	Ni	Pb	Bi	Te	Total
Sobolevskite							
NCN-B53-1an1	30.33	1.28	n.a.	b.d.l.	67.97	b.d.l.	99.58
NCN-B53-2an1	29.16	1.47	n.a.	b.d.l.	64.58	b.d.l.	95.21
NCN-B53-3an1	33.38	2.92	n.a.	b.d.l.	64.50	b.d.l.	100.80
NCN-A53-1an1	31.49	3.72	n.a.	b.d.l.	68.28	b.d.l.	103.49
NCN-C53-1an1	32.13	1.94	n.a.	b.d.l.	65.49	b.d.l.	99.55
NCN-C53-1an2	33.41	1.72	n.a.	b.d.l.	65.78	b.d.l.	100.91
NCN-C53-1an3	32.31	1.87	n.a.	b.d.l.	66.22	b.d.l.	100.40
NCN-C53-2an1	31.11	2.15	n.a.	b.d.l.	64.35	b.d.l.	97.61
NCN-Bminus53-1an1	33.65	3.62	0.73	b.d.l.	63.07	b.d.l.	101.08
NCN-Aminus53-1an1	31.77	3.22	0.78	b.d.l.	63.88	b.d.l.	99.65
NCN-Fminus53-1an1	32.59	2.34	0.38	b.d.l.	64.69	b.d.l.	100.00
Bi-rich kotulskite							
NCN-Bminus53-an2	39.23	1.07	0.26	b.d.l.	29.37	28.83	98.77

At%	Pd	Fe	Ni	Pb	Bi	Te	Total
Sobolevskite							
NCN-B53-1an1	45.01	3.62	n.a.	b.d.l.	51.36	b.d.l.	100
NCN-B53-2an1	44.98	4.31	n.a.	b.d.l.	50.71	b.d.l.	100
NCN-B53-3an1	46.50	7.74	n.a.	b.d.l.	45.76	b.d.l.	100
NCN-A53-1an1	42.92	9.67	n.a.	b.d.l.	47.40	b.d.l.	100
NCN-C53-1an1	46.45	5.34	n.a.	b.d.l.	48.22	b.d.l.	100
NCN-C53-1an2	47.60	4.67	n.a.	b.d.l.	47.73	b.d.l.	100
NCN-C53-1an3	46.43	5.11	n.a.	b.d.l.	48.46	b.d.l.	100
NCN-C53-2an1	45.77	6.02	n.a.	b.d.l.	48.21	b.d.l.	100
NCN-Bminus53-1an1	45.49	9.33	1.76	b.d.l.	43.42	b.d.l.	100
NCN-Aminus53-1an1	44.23	8.53	1.95	b.d.l.	45.29	b.d.l.	100
NCN-Fminus53-1an1	46.12	6.31	0.95	b.d.l.	46.62	b.d.l.	100
Bi-rich kotulskite							
NCN-Bminus53-an2	48.59	2.52	0.58	0.00	18.53	29.78	

apfu	Pd	Fe	Ni	Pb	Bi	Te	Total
Sobolevskite							
NCN-B53-1an1	0.90	0.07	n.a.	b.d.l.	1.03	0.00	2
NCN-B53-2an1	0.90	0.09	n.a.	b.d.l.	1.01	0.00	2
NCN-B53-3an1	0.93	0.15	n.a.	b.d.l.	0.92	0.00	2
NCN-A53-1an1	0.86	0.19	n.a.	b.d.l.	0.95	0.00	2
NCN-C53-1an1	0.93	0.11	n.a.	b.d.l.	0.96	0.00	2
NCN-C53-1an2	0.95	0.09	n.a.	b.d.l.	0.95	0.00	2

NCN-C53-1an3	0.93	0.10	n.a.	b.d.l.	0.97	0.00	2
NCN-C53-2an1	0.92	0.12	n.a.	b.d.l.	0.96	0.00	2
NCN-Bminus53-1an1	0.91	0.19	0.04	b.d.l.	0.87	0.00	2
NCN-Aminus53-1an1	0.88	0.17	0.04	b.d.l.	0.91	0.00	2
NCN-Fminus53-1an1	0.92	0.13	0.02	b.d.l.	0.93	0.00	2
Bi-rich kotulskite							
NCN-Bminus53-an2	4.86	0.25	0.06	b.d.l.	1.85	2.98	10

n.a. = not analyzed, b.d.l. = below detection limit.